



Contents lists available at ScienceDirect

Indian Pacing and Electrophysiology Journal

journal homepage: www.elsevier.com/locate/IPEJ

Local impedance-guided ablation and ultra-high density mapping versus conventional or contact force-guided ablation with mapping for treatment of cavotricuspid isthmus dependent atrial flutter

Karan Saraf^{a, b}, Nicholas Black^{a, c}, Clifford J. Garratt^{a, b}, Sahrkaw A. Muhyaldeen^b, Gwilym M. Morris^{a, b, *}

^a Division of Cardiovascular Sciences, The University of Manchester, Oxford Road, Manchester, M139PL, UK

^b Manchester Heart Centre, Manchester University NHS Foundation Trust, Oxford Road, Manchester, M139WL, UK

^c Royal Oldham Hospital, Rochdale Road, Oldham, OL1 2JH, UK



ARTICLE INFO

Article history:

Received 10 December 2021

Received in revised form

1 March 2022

Accepted 30 March 2022

Available online 12 April 2022

Keywords:

Atrial flutter

Ablation

Local impedance

Ultra-high density mapping

ABSTRACT

Introduction: – Local impedance (LI) guided ablation as a method of judging lesion effectiveness for cavotricuspid isthmus dependent atrial flutter (CTI-AFL), and ultra-high density (UHD) mapping when breakthrough occurred across an ablation line has not previously been assessed.

Methods: This retrospective observational study evaluated patients undergoing CTI-AFL ablation using conventional, contact force (CF) and LI guided strategies. Ablation metrics were collected, and in the LI cohort, the use of UHD mapping for breakthrough evaluated.

Results: 30 patients were included, 10 per group. Mean total ablation time was significantly shorter with LI (3.2 ± 1.3 min) vs conventional (5.6 ± 2.7 min) and CF (5.7 ± 2.0 min, $p = 0.0042$). Time from start of ablation to CTI block was numerically shorter with LI (14.2 ± 8.0 min) vs conventional and CF (19.7 ± 14.1 and 22.5 ± 19.1 min, $p = 0.4408$). Mean lesion duration was significantly shorter with LI, but there were no differences in the number of lesions required to achieve block, procedural success, complication rates or recurrence. 15/30 patients did not achieve block following first-pass ablation. UHD mapping rapidly identified breakthrough in the five LI patients, including epicardial-endocardial breakthrough (EEB).

Conclusion: – The use of LI during ablation for real-time lesion assessment was as efficacious as the conventional and CF methods. UHD mapping rapidly identified breakthrough, including EEB.

© 2022 Indian Heart Rhythm Society. Published by Elsevier B.V. This is an open access article under the CC BY-NC-ND license (<http://creativecommons.org/licenses/by-nc-nd/4.0/>).

1. Introduction

Cavotricuspid isthmus dependent atrial flutter (CTI-AFL), also known as typical atrial flutter, describes a macroreentrant circuit around the tricuspid valve annulus, with conduction through the CTI being a prerequisite for arrhythmia maintenance. The overall incidence in the general population is approximately 0.9% [1]. Radiofrequency (RF) catheter ablation of the CTI is the most effective treatment for this condition, with a single-procedure success rate of 95% and is a class I recommendation from the European Society of Cardiology [2,3]. Ablation is performed along the CTI

from the tricuspid annulus to the inferior vena cava (IVC) and successful outcome achieved when bi-directional conduction block is present across the ablation line. When this endpoint is met, recurrence rates are approximately 5%, with recurrence occurring when functional gaps are present within the ablation line, or when epicardial-endocardial breakthrough (EEB) occurs due to bridging epicardial fibres across the CTI [2,4,5].

The conventional technique involves the use of bipolar intracardiac electrograms (EGMs), fluoroscopic image guidance and radiofrequency generator impedance to position catheters prior to applying RF. Due to the trabeculated and heterogeneous anatomy of the CTI, it can be difficult to achieve a contiguous ablation line using only these metrics, resulting in extensive ablation and significant radiation exposure to both patient and operator [4,6].

Interest in optimising catheter-tissue contact and real-time metrics of effective ablation lesion delivery has resulted in the development of new technology to this end. A number of studies

* Corresponding author. Division of Cardiovascular Sciences, The University of Manchester, Oxford Road, Manchester M139PL, UK.

E-mail address: Gwilym.morris@manchester.ac.uk (G.M. Morris).

Peer review under responsibility of Indian Heart Rhythm Society.

have evaluated contact force (CF, using the Thermocool SmartTouch ablation catheter; Biosense Webster, Diamond Bar CA, USA) or electrical coupling index (Ensite Verisense ECI ablation catheter; St Jude Medical, St Paul MN, USA) to improve assessment of catheter–tissue contact prior to RF energy delivery [7–10]. Recently, catheters that measure local tissue impedance (LI) have been developed (IntellaNav MiFi; Boston Scientific, Marlborough MA, USA) allowing measurement of tissue contact as well as a direct metric of lesion formation via the reduction in LI values. In vitro and in vivo studies have validated LI as a valuable measure of catheter-tissue contact, and have also shown a reduction in LI during application of RF to correspond to effective lesion formation [11–13].

The use of adequate LI reduction as a target endpoint for lesion formation has not yet been evaluated against the routinely used conventional or contact force-guided ablation for CTI-AFL in humans. We conducted a pilot study to assess LI-guided ablation as a measure of lesion effectiveness at the CTI, and whether ultra-high density 3D electro-anatomic mapping could be used to identify and characterise the nature of breakthrough at a CTI ablation line.

2. Methods

This retrospective observational pilot study compared patients undergoing clinically indicated radiofrequency ablation of CTI-dependent AFL with fluoroscopic guided ablation (conventional group), CF-guided ablation with 3-dimensional (3D) electro-anatomic mapping (Carto-3, Biosense-Webster, CF group), and LI-guided ablation and ultra-high density (UHD) mapping (Rhythmia HDx, Boston Scientific, LI group). Patients were eligible for inclusion if they were aged greater than 18 years old undergoing first-time ablation of suspected CTI-AFL, either alone or as part of another ablation procedure.

Procedures took place between 11th December 2018 and 5th October 2020 at a single tertiary cardiac centre by four experienced cardiac electrophysiologists familiar with all three technologies. The methods described in this section correspond to local procedural guidelines. Procedures were performed under local anaesthesia and conscious sedation or general anaesthetic. Intravascular access was obtained using left or right femoral veins. Oral anticoagulation (warfarin or direct oral anticoagulant) was continued peri-procedurally. A decapolar catheter was inserted into the coronary sinus. The use of a right atrial 20-pole “halo” diagnostic catheter (Biosense Webster) occurred in all patients. The creation of 3D right atrial anatomy and activation mapping (LI and CF groups) was left to operator discretion, as was the use of steerable sheath if satisfactory contact or stability could not be achieved.

A CTI ablation line was created using a point-by-point approach. At each point, irrigated RF was delivered, guided by 5 Ω reduction in generator impedance, intracardiac bipolar electrogram attenuation $\geq 50\%$ and/or development of local split potentials at operator discretion (conventional and CF groups), or until a target LI drop was achieved (LI group, see below) up to a maximum of 60 s per lesion (all groups). For all groups, the power was limited to 40–50W depending on operator preference, with a maximum temperature of 48 °C and flow of 30 ml/min as per manufacturer recommendations. Catheters used were Thermocool and Thermocool SmartTouch (Biosense Webster) for conventional and CF groups respectively, and IntellaNav MiFi (Boston Scientific) for the LI group.

For the CF-guided cohort, a contact force of 9–40 g was targeted for each lesion. If bi-directional CTI block was not obtained following first-pass ablation, additional lesions were delivered at breakthrough gaps and 3D mapping could be performed at operator discretion to identify sites of breakthrough to target for further

ablation.

For the LI-guided group, contact was determined using patient-specific LI measurement by comparing tissue contact LI against blood pool impedance, aiming for a starting contact impedance of 110–130 Ω . RF was applied until a target LI reduction of 20 Ω was achieved (likely successful lesion) or a plateau of at least 2 s was reached following an initial LI drop. If bi-directional CTI block was not obtained following first-pass ablation, additional lesions were delivered at breakthrough gaps, with UHD mapping utilised at operator discretion to identify and characterise the nature of the breakthrough target for further ablation (Intellamap Orion; Boston Scientific).

Confirmation of bi-directional CTI block was obtained using standard multi-site pacing manoeuvres. Following confirmation of bi-directional block, an observation period of 30 min was carried out, to exclude recovery of conduction across the ablation line. Patients received clinically indicated follow up at 3-, 6-, and 12-months post-procedure, with a 12-lead ECG at the time of review to ensure maintenance of sinus rhythm, and further ambulatory ECG monitoring was performed if symptoms suggestive of possible arrhythmia recurrence were reported.

Data collected included total RF time, time from first application of RF to confirmation of bi-directional CTI block, number of lesions required to achieve block and mean lesion duration. For CF-guided cases, measurements for maximum, minimum and mean CF, and mean force-time integral (FTI) values per lesion were collected (FTI values were collected post-procedurally and were not used to guide ablation due to lack of validation in CTI ablation). For LI-guided cases, mean starting LI and mean LI drop was measured. Acute procedural success, procedural complications, the requirement for re-ablation and duration of follow up were also assessed. Analysis was performed using ANOVA for parametric data, with multiple comparisons ANOVA between groups corrected using the two-stage step-up method, or the Kruskal-Wallis test for non-parametric data. The chi-square or Fisher exact test was used for categorical variables. All statistical analysis was performed using Prism version 9.0 (GraphPad Software, San Diego CA, USA).

In cases where bi-directional block was not achieved following first-pass ablation, to allow analysis of breakthrough, division of the CTI into three segments was required - adjacent to the tricuspid valve annulus (TV-CTI), the mid-portion (mid-CTI) and adjacent to the inferior vena cava (IVC-CTI). Breakthrough points were grouped according to their location within these segments.

3. Results

3.1. Baseline characteristics

30 consecutive patients were included – ten in each of the three groups – conventional, contact force- and local impedance-guided ablation. There were no significant differences between the three groups in age or prevalence of common cardiovascular comorbidities (Table 1), and there was significant male preponderance overall (86.7%). All patients who underwent conventional ablation had CTI ablation only, whilst five of ten patients undergoing CF-guided and one of ten patients undergoing LI-guided ablation had CTI ablation as part of a procedure in which they also underwent pulmonary vein isolation for atrial fibrillation (AF).

3.2. Outcome measures

The mean (\pm standard deviation) total ablation time (cumulative time that RF was applied) was 5.6 ± 2.7 min for conventional, 5.7 ± 2.0 min for CF-guided and 3.2 ± 1.3 min for LI-guided ablation ($p = 0.0042$). Statistically significant differences were also seen

Table 1
Baseline characteristics.

	Conventional n = 10	CF-guided n = 10	LI-guided n = 10	p value
Age (SD)	69.7 (8.2)	61.3 (8.6)	66.0 (11.1)	p = 0.123
Male gender (%)	10 (100)	9 (90)	7 (70)	p = 0.133
Co-existing AF (%)	4 (40)	6 (60)	5 (50)	p = 0.670
Diabetes mellitus (%)	2 (20)	2 (20)	1 (10)	p = 0.787
IHD (%)	3 (30)	4 (40)	1 (10)	p = 0.303
HTN (%)	2 (20)	1 (10)	2 (20)	p = 0.787
LVSD (%)	4 (40)	5 (50)	4 (40)	p = 0.873

AF, atrial fibrillation; IHD, ischaemic heart disease; HTN, hypertension; LVSD, left ventricular systolic dysfunction; SD, standard deviation.

individually between LI and conventional ($p = 0.0058$) and between LI and CF groups ($p = 0.0031$; Fig. 1A). The mean time taken from first application of RF to confirmation of bi-directional CTI block (the time at which the final lesion was delivered prior to confirmation of block) was 19.7 ± 14.1 min for conventional, 22.5 ± 19.1 min for CF and 14.2 ± 8.0 min for LI-guided ablation ($p = 0.4408$; Fig. 1B). The number of lesions required to achieve block was 9.2 ± 3.5 for conventional, 12.6 ± 6.5 for CF-guided and 8.0 ± 2.5 for LI-guided groups ($p = 0.0769$; Fig. 1C), and the mean lesion duration was 38.4 ± 13.6 s for conventional, 33.3 ± 14.6 s for CF-guided and 23.8 ± 5.1 s for LI-guided ($p = 0.0132$, Fig. 1D). For CF-guided cases, mean contact force was $15.3g \pm 3.6g$, with a mean maximum CF value of $24.5g \pm 5.5g$, mean minimum CF value of $9.2g \pm 2.0g$, and mean FTI of 515.6 ± 280.2 gs. Mean starting LI was $112.7 \pm 13.6\Omega$ and mean LI drop was $21.2 \pm 7.8\Omega$ for LI-guided cases. There was 100% acute procedural success, no reported procedural complications and no requirement for repeat ablation during the follow-up period for all three groups (14.6 ± 8.5 months for

conventional, 15.1 ± 8.8 months for CF and 9.9 ± 4.6 months for LI; $p = 0.2394$).

3.3. Second-pass lesion set

First-pass bi-directional block was not achieved in four conventional, six CF and five LI patients ($p = 0.6703$). The ablation parameters of the second-pass lesion set were analysed. Total ablation time was 1.9 ± 0.6 min for conventional, 1.2 ± 0.3 min for CF and 0.8 ± 0.5 min for LI ($p = 0.0531$; Fig. 1E). The time taken from starting the second-pass lesion set and confirmation of CTI block was 4.7 ± 3.2 min for conventional, 2.3 ± 1.1 min for CF and 1.2 ± 0.9 min for LI ($p = 0.0609$; Fig. 1F). The additional lesions required to achieve CTI block were 3.8 ± 3.6 for conventional, 2.8 ± 0.4 for CF and 1.8 ± 1.0 for LI ($p = 0.3850$; Fig. 1G), and the mean lesion duration was 44.4 ± 20.4 s for conventional, 26.2 ± 5.3 s for CF and 27.2 ± 6.7 s for LI ($p = 0.0758$; Fig. 1H).

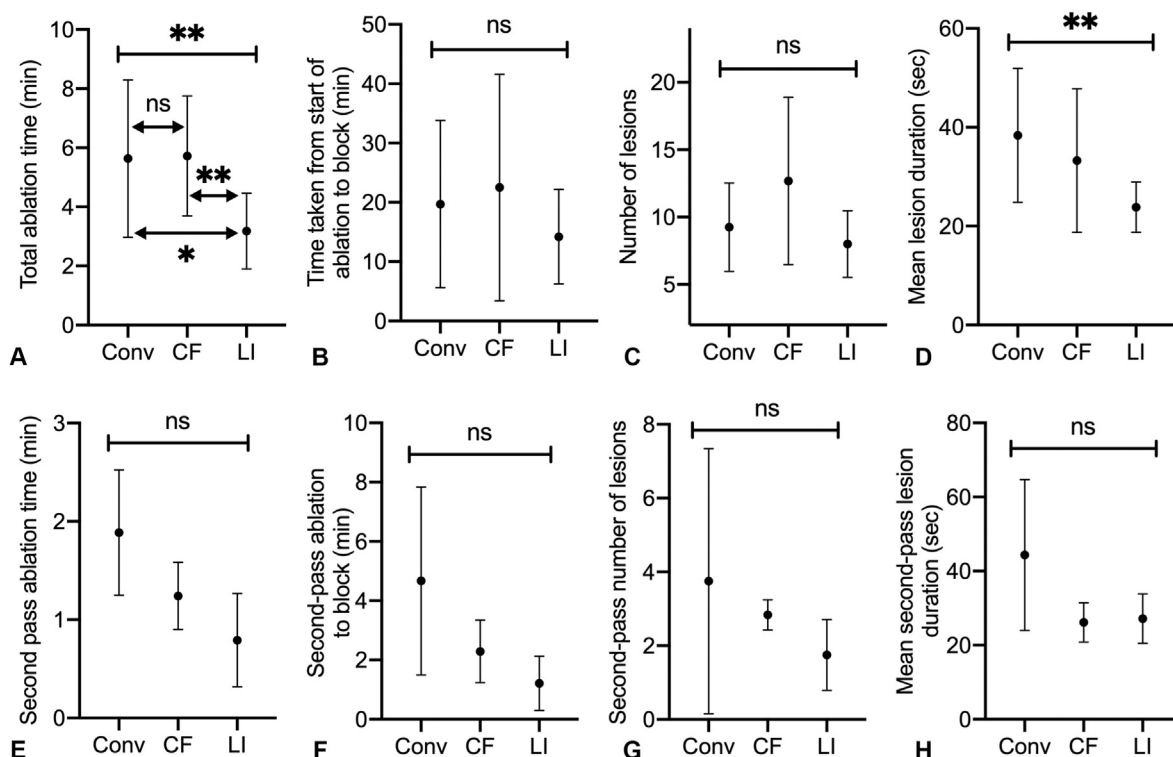


Fig. 1. Graphs of ablation metric outcomes. Graphs showing overall mean ablation metrics (panels A–D) and second pass ablation metrics (panels E–H). Dots and bars represent mean and standard deviation respectively. A. Total radiofrequency ablation time. B. Time taken from first application of radiofrequency ablation to confirmation of bi-directional cavotricuspid isthmus block. C. Number of lesions required to achieve bi-directional block. D. Mean duration of radiofrequency for each lesion. E. Total second-pass radiofrequency ablation time. F. Time taken from start of second-pass ablation to confirmation of bi-directional cavotricuspid isthmus block. G. Number of lesions in the second-pass lesion set. H. Mean duration of radiofrequency for each lesion in the second-pass lesion set. * = $p < 0.05$, ** = $p < 0.005$, ns = non-significant ($p > 0.05$). Conv, conventional; CF, contact force; LI, local impedance.

3.4. Sites of acute breakthrough

None of the patients in the CF group had 3D mapping, whilst all five in the LI group underwent UHD mapping of the CTI following failure of first-pass ablation to identify the precise location and nature of breakthrough (Fig. 2). The mean length of the CTI in these patients was 35.2 ± 2.8 mm. Four patients had linear breakthrough at the CTI; one patient 4.2 mm from the tricuspid valve annulus (within the TV-CTI segment, Fig. 3), and three between 20.2 and 29.8 mm from the TV annulus (within the IVC-CTI segment). In one patient the breakthrough was away from the ablation line, 10.4 mm lateral to the mid-CTI, representing epicardial-endocardial breakthrough (EEB; Fig. 4A and B).

4. Discussion

This pilot study demonstrates that LI guided ablation provides comparable success rates to conventional and CF-guided ablation, and may reduce total ablation time by shortening the time for each lesion delivered. Breakthrough across the initial ablation line characterised by UHD mapping achieved block with numerically fewer ablation lesions than conventional and CF-guided ablation.

CF-sensing catheters have been validated as a robust way to assess the catheter-tissue interface and deliver lesions with lower rates of dormant conduction and electrical reconnection than catheters lacking this information [8–10,14,15]. The Thermocool SmartTouch catheter used in this study provides a direct measurement of the force applied by the catheter on the endocardium (displayed as grams), but does not measure tissue viability. This method, however, does not take into account real-time or

physiological information about the catheter-tissue interface during the application of radiofrequency. The IntellaNav MiFi catheter can provide real-time information about the catheter-tissue interface and physiological tissue properties. It uses a local potential field generated by three miniature electrodes at the catheter tip to measure local resistivity and therefore local impedance, rather than generator impedance used in other systems. Healthy tissue displays greater resistivity and LI ($110 \pm 13.7\Omega$) than the surrounding blood pool ($91.9 \pm 9.9\Omega$), providing the operator with some semi-quantitative information about catheter-tissue contact. An ex vivo study evaluating LI and CF showed 141–144 Ω to be equivalent to 31.5g (IQR 27–52g) of contact force [11,12]. A patient-specific baseline local impedance for healthy tissue and blood pool are observed prior to RF application, for tissue by placing the catheter against the endocardium in multiple locations, with stability judged by tactile feedback, local electrograms and voltage, and for blood pool by placing the catheter in a cardiac chamber and confirming an absence of electrograms recorded by the catheter. A reduction from a baseline LI during RF application has been validated as an accurate measure of resistive heating and formation of transmural lesions [12,16]. Clinical studies in the human left atrium and both ventricles have shown successful lesions to be correlated with a mean LI drop of 14.6 Ω and 16–18 Ω respectively [11,13]. A subsequent study specifically looking at LI targets for CTI ablation showed a 12 Ω drop to be sufficient to create effective lesions at the CTI [17]. The mean LI drop of $21.2 \pm 7.8\Omega$ in this study shows that a target LI drop of 20 Ω at the CTI is a valid strategy with comparable success rates to CF or conventional methods.

Using LI guided ablation may allow shortening of the ablation time by reducing unnecessary ablation once a successful lesion has been delivered. In this study, the total ablation time was significantly reduced with an LI guided strategy. Similarly, the Ensite Verisense ECI catheter (St Jude Medical) that provides information on tissue viability using a measure of electrical coupling (electrical coupling index, ECI) reduced the time to CTI block from 30.0 to 10.5 min in the VERISMART trial, demonstrating that using physiological tissue parameters may offer benefits over CF measurement alone [7].

4.1. Ablation metrics

Total RF time in the LI cohort was significantly reduced compared to the other two groups ($p = 0.0042$). These differences were also individually statistically significant, with a 43% reduction versus conventional ($p = 0.0058$) and a 44% reduction versus CF ($p = 0.0031$). The mean lesion duration was also significantly shorter for LI-guided ablation ($p = 0.0132$). This shorter duration suggests that on the CTI, effective lesion formation guided by LI drop may allow a reduction in RF time without a reduction in acute success. Further corroboration of this can be observed by the fact that there was no significant difference between the groups in the total number of ablation lesions, suggesting that RF delivery guided by LI change during lesion formation shortened the required duration of each lesion. The operator is able to use this extra real-time information and stop ablating once a significant LI drop has been observed and move on to creating the next lesion, rather than relying on only generator impedance and electrogram attenuation, as with the conventional and CF-guided methods. This benefit was maintained against good force in the CF group, as mean CF measurement during CF-guided ablation was $15.3 \pm 3.6g$, reflecting good catheter-tissue contact, and although target FTI values have not been validated for ablation at the CTI, the mean FTI of 515.6 ± 280.2 gs also suggests good lesion formation in the CF cohort when compared with studies evaluating left atrial ablation [18,19].

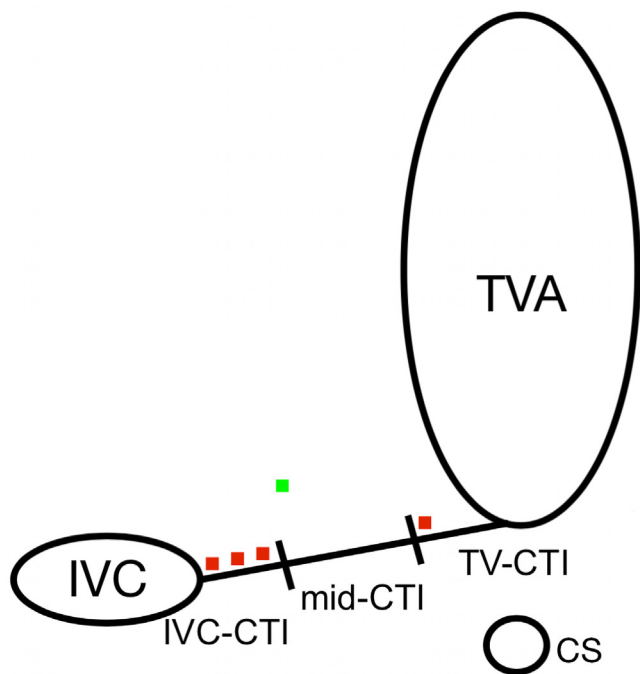


Fig. 2. Simplified diagram of the cavotricuspid isthmus showing sites of breakthrough following first-pass ablation in right anterior oblique orientation. The isthmus has been divided into three segments, based on proximity to TV, IVC or the mid-portion. Red points represent breakthrough across the line, green point shows epicardial-endocardial breakthrough lateral to line. TVA, tricuspid valve annulus; IVC, inferior vena cava; CS, coronary sinus ostium; CTI, cavotricuspid isthmus.

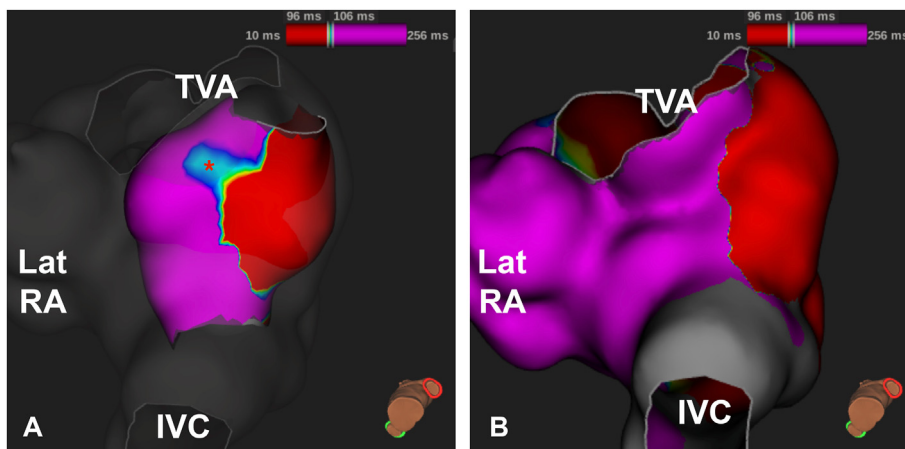


Fig. 3. Ultra-high density 3-dimensional electroanatomic right atrial maps of the cavotricuspid isthmus (CTI) ablation line in a patient from the local impedance cohort, in left anterior oblique caudal view. There is breakthrough across the tricuspid aspect of the ablation line (panel A, red asterisk). Targeted ablation at this point resulted in bi-directional CTI block as shown in panel B. Timing is shown from the pacing electrode in the proximal coronary sinus and is displayed at the same timing in both maps; the activation wavefront is between 96 ms and 106 ms after pacing. TVA, tricuspid valve annulus; IVC, inferior vena cava; Lat RA, lateral right atrium.

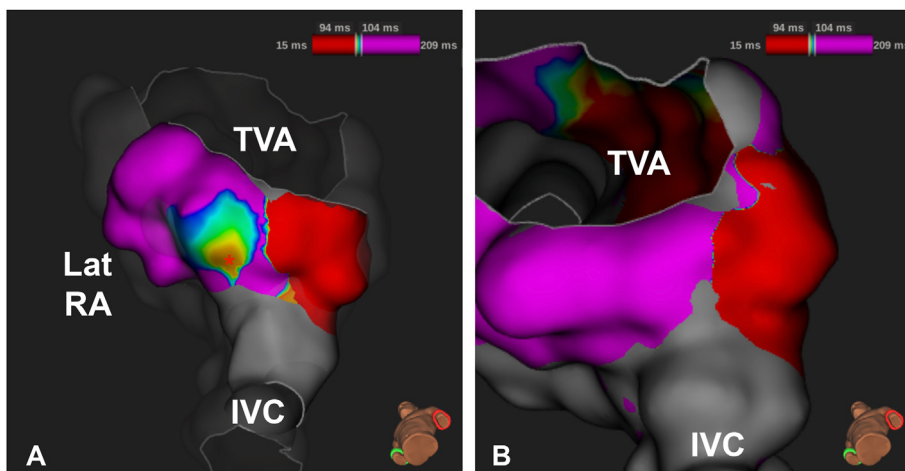


Fig. 4. Ultra-high density 3-dimensional electroanatomic right atrial maps of the cavotricuspid isthmus (CTI) ablation line in a patient from the local impedance cohort, in left anterior oblique caudal view. There is epicardial-endocardial breakthrough 10.4 mm lateral to the cavotricuspid isthmus (CTI) ablation line, displaying radial spread (panel A, red asterisk). Targeted ablation at this point resulted in bi-directional CTI conduction block as shown in panel B. Timing is shown from the pacing electrode in the coronary sinus and is displayed at the same timing in both maps; the activation wavefront is between 94 ms and 104 ms after pacing. TVA, tricuspid valve annulus; IVC, inferior vena cava; Lat RA, lateral right atrium.

There was a numerical reduction in time from the first application of RF to confirmation of bi-directional CTI block using LI-guided ablation compared with conventional and CF groups, although this was statistically non-significant.

First-pass ablation did not result in bi-directional CTI block in similar numbers of patients in each group. Although numerical reductions were seen in the second-pass lesion set with LI-guided ablation, in total ablation time, from the start of lesion set to confirmation of CTI block, and the number of lesions required in second-pass ablation, these differences were statistically non-significant. There were no differences between rates of complication or procedural success, defined by patient-reported symptoms and 12-lead ECG performed at the time of follow-up.

CF and LI sensing catheters measure the catheter-tissue interface in different ways. The baseline LI measurement can give the operator some idea about tissue contact, as the blood pool displays

lower impedance than the endocardium ($91.9 \pm 9.9\Omega$ for blood pool versus $110 \pm 13.7\Omega$ for endocardium from a previous study, with mean baseline LI of endocardium in our analysis of $112.7 \pm 13.6\Omega$), although does not provide absolute force measurements like CF catheters. Real-time LI data during ablation may reduce lesion duration and total RF time, although the small numbers evaluated in this study do not allow for definitive conclusions.

4.2. Analysis of breakthrough

In this study, UHD mapping was used to identify sites of breakthrough in the LI cohort when first-pass isthmus block was not achieved. Fig. 3 shows a UHD map of one case with breakthrough across the CTI. A single further ablation lesion at this point resulted in bi-directional CTI block. In another case, breakthrough was identified 10.4 mm lateral to the CTI ablation line, with

activation mapping showing outward radial spread from this point, with a unipolar rS pattern seen at the point of breakthrough, and identical activation timing on each pacing cycle length, representing epicardial-endocardial breakthrough. Further ablation at the point of the breakthrough resulted in bi-directional isthmus block in this patient (Fig. 4).

Histological analysis of the CTI has shown it to be heterogeneous in its anatomy, receiving muscle fibres from the crista terminalis of varying number and morphology, separated by connective tissue. The TV segment is smooth, the mid-CTI is the most trabeculated, owing to the extensions of the pectinate muscles, and the IVC segment consists of fibro-fatty tissue [20,21]. It could be postulated that breakthrough is most likely to occur in the mid-CTI as trabeculation can increase the difficulty of obtaining contact and transmural ablation. However in this study, three of four linear breakthrough points occurred at the IVC-CTI, with the other at the TV-CTI. The presence of a prominent Eustachian ridge or pouch in the IVC-CTI may cause difficulties in achieving effective ablation, and this may have accounted for breakthrough in these patients. In some cases, ablation lateral or medial to areas of breakthrough may be required if the underlying anatomy makes it difficult to achieve a contiguous lesion set [22]. In the LI cases, further ablation at the points of breakthrough identified by UHD mapping resulted in bi-directional block, but it is possible that in the other two groups without the aid of mapping, some variation in the plane of ablation line was adopted (medial or lateral to the first-pass line) in order to achieve block, and although statistically non-significant, there was a reduction in the number of additional lesions required.

Intraoperative mapping studies have shown that EEB can be critical to the maintenance of human persistent AF [23,24]. The development of UHD mapping provides an opportunity to study atrial endocardial activation patterns to a level of detail not previously possible. One study by Pathik et al. observed and confirmed the presence of EEB in 14/26 patients undergoing ablation for CTI-AFL [5]. In all cases, EEB was present adjacent to a line of block, either occurring naturally in the RA (mostly in the posterior RA adjacent to the posterior line of block) during stable macroreentry, or near a successfully ablated CTI, and in several cases was a critical feature of the tachycardia. Sites of breakthrough were 13.4–19.4 mm from the adjacent lines of block; in the case of EEB occurring medially to the CTI during counter-clockwise macroreentrant flutter, a single application of RF at this site resulted in the termination of tachycardia. The case of EEB in this study was located 10.4 mm lateral to the mid-CTI and to our knowledge, the first case of EEB uncovered during coronary sinus pacing. The heterogeneous muscle bundle arrangement at the CTI may contribute to the differential activation between epi- and endocardium and the formation of EEB within the vicinity of the CTI; in cases where epicardial fibres bridge the CTI, EEB may only be exposed following ablation creating a line of block.

Whilst there have been no studies systematically looking at EEB as a potentially significant factor in the failure to achieve CTI block, its description in case reports, the regularity with which Pathik et al. observed this phenomenon using UHD mapping, and its association with lines of block, it is possible that with further investigation it may be more frequently implicated in cases of treatment failure. The use of UHD mapping may help to rapidly identify sites of breakthrough, including EEB and target ablation if the initial procedure has been unsuccessful [5,25,26].

5. Limitations

Given the retrospective nature of this study, and small numbers involved, definitive conclusions regarding these ablation methods cannot be made.

6. Conclusion

This pilot study shows that LI-guided ablation is at least as successful and safe as conventional and CF-guided ablation for CTI dependent atrial flutter, and may have some theoretical benefits in ablation metrics. Ultra-high density mapping was seen to rapidly identify sites of breakthrough following the first-pass ablation line, which was unsuccessful in 5/10 patients in the LI cohort (compared with similar numbers of first-pass failure in the other groups), and this may have contributed towards the reduced ablation time observed in the LI group. A larger multi-centre prospective randomised study with appropriate power is planned.

Declarations

Karan Saraf, Nicholas Black, Clifford Garratt, Sahrkaw Muhyaldeen and Gwilym Morris take responsibility for all aspects of the reliability and freedom from bias of the data presented and their discussed interpretation.

Funding

None.

Authors' contributions

All authors contributed towards the conception, analysis and writing as per ICMJE recommendations.

Ethics approval

N/A.

Declaration of competing interest

Karan Saraf: research funding from Boston Scientific.
 Nicholas Black: None.
 Clifford J Garratt: None.
 Sahrkaw Muhyaldeen: sponsorship for conference attendance from Biosense Webster.
 Gwilym M Morris: research funding from Boston Scientific, Honoraria from Boston Scientific and Biosense Webster.

References

- [1] Granada J, Uribe W, Chyou P-H, Maassen K, Vierkant R, Smith PN, et al. Incidence and predictors of atrial flutter in the general population. *J Am Coll Cardiol* 2000;36(7):2242–6.
- [2] Kirchhof P, Benussi S, Kotecha D, Ahlsson A, Atar D, Casadei B, et al. ESC Guidelines for the management of atrial fibrillation developed in collaboration with EACTS. *Eur Heart J* 2016;37(38):2893–962. 2016.
- [3] Natale A, Newby KH, Pisano E, Leonelli F, Fanelli R, Potenza D, et al. Prospective randomized comparison of antiarrhythmic therapy versus first-line radiofrequency ablation in patients with atrial flutter. *J Am Coll Cardiol* 2000;35:1898–904.
- [4] Willems S, Weiss C, Ventura R, Ruppel R, Risius T, Hoffman M, et al. Catheter ablation of atrial flutter guided by electroanatomic mapping (CARTO): a randomized comparison to the conventional approach. *J Cardiovasc Electro-physiol* 2000;11(11):1223–30.
- [5] Pathik B, Lee G, Sacher F, Haissaguerre M, Jais P, Massoulié G, et al. Epicardial-endocardial breakthrough during stable atrial macroreentry: evidence from ultra-high-resolution 3-dimensional mapping. *Heart Rhythm* 2017;14(8):1200–7.
- [6] Kottkamp H, Hugl B, Krauss B, Wetzel U, Fleck A, Schuler G, et al. Electro-magnetic versus fluoroscopic mapping of the inferior isthmus for ablation of typical atrial flutter: a prospective randomised study. *Circulation* 2000;102:2082–6.
- [7] Begg GA, O'Neill J, Sohaib A, McLean A, Pepper CB, Graham LN, et al. Multi-centre randomised trial comparing contact force with electrical coupling index in atrial flutter ablation (VERISMART trial). *PLoS One* 2019;14(4):e0212903.

- [8] Haldar S, Jarman JW, Panikker S, Jones DG, Salukhe T, Gupta D, et al. Contact force sensing technology identifies sites of inadequate contact and reduces acute pulmonary vein reconnection: a prospective case control study. *Int J Cardiol* 2013;168(2):1160–6.
- [9] Neuzil P, Reddy VY, Kautzner J, Petru J, Wichterle D, Shah D, et al. Electrical reconnection after pulmonary vein isolation is contingent on contact force during initial treatment: results from the EFFICAS I study. *Circ Arrhythm Electrophysiol* 2013;6(2):327–33.
- [10] Kuck KH, Reddy VY, Schmidt B, Natale A, Neuzil P, Saoudi N, et al. A novel radiofrequency ablation catheter using contact force sensing: toccata study. *Heart Rhythm* 2012;9(1):18–23.
- [11] Munkler P, Gunawardene MA, Jungen C, Klatt N, Schwarzl JM, Akbulak RO, et al. Local impedance guides catheter ablation in patients with ventricular tachycardia. *J Cardiovasc Electrophysiol* 2020;31(1):61–9.
- [12] Sulkin MS, Laughner JI, Hilbert S, Kapa S, Kosiuk J, Younan P, et al. Novel measure of local impedance predicts catheter-tissue contact and lesion formation. *Circ Arrhythm Electrophysiol* 2018;11(4):e005831.
- [13] Martin CA, Martin R, Gajendragadkar PR, Maury P, Takigawa M, Cheniti G, et al. First clinical use of novel ablation catheter incorporating local impedance data. *J Cardiovasc Electrophysiol* 2018;29(9):1197–206.
- [14] Andrade JG, Monir G, Pollak SJ, Khairy P, Dubuc M, Roy D, et al. Pulmonary vein isolation using "contact force" ablation: the effect on dormant conduction and long-term freedom from recurrent atrial fibrillation—a prospective study. *Heart Rhythm* 2014;11(11):1919–24.
- [15] Shurrab M, Di Biase L, Briceno DF, Kaoatskaia A, Haj-Yahia S, Newman D, et al. Impact of contact force technology on atrial fibrillation ablation: a meta-analysis. *J Am Heart Assoc* 2015;4(9):e002476.
- [16] Gunawardene M, Munkler P, Eickholt C, Akbulak RO, Jularic M, Klatt N, et al. A novel assessment of local impedance during catheter ablation: initial experience in humans comparing local and generator measurements. *Europace* 2019;21(Supplement_1):i34–42.
- [17] Sasaki T, Nakamura K, Inoue M, Minami K, Miki Y, Goto K, et al. Optimal local impedance drops for an effective radiofrequency ablation during cavotricuspid isthmus ablation. *J Arrhythm* 2020;36(5):905–11.
- [18] Squara F, Latcu DG, Massaad Y, Mahjoub M, Bun SS, Saoudi N. Contact force and force-time integral in atrial radiofrequency ablation predict transmuralty of lesions. *Europace* 2014;16(5):660–7.
- [19] Kumar S, Morton JB, Lee J, Halloran K, Spence SJ, Gorelik A, et al. Prospective characterization of catheter-tissue contact force at different anatomic sites during antral pulmonary vein isolation. *Circ Arrhythm Electrophysiol* 2012;5(6):1124–9.
- [20] Ho S. Atrial structure and fibres: morphologic bases of atrial conduction. *Cardiovasc Res* 2002;54(2):325–36.
- [21] Cabrera JA, Sanchez-Quintana D, Farre J, Rubio JM, Ho SY. The inferior right atrial isthmus: further architectural insights for current and coming ablation technologies. *J Cardiovasc Electrophysiol* 2005;16(4):402–8.
- [22] Christopoulos G, Siontis KC, Kucuk U, Asirvatham SJ. Cavotricuspid isthmus ablation for atrial flutter: anatomic challenges and troubleshooting. *Heart-Rhythm Case Rep* 2020;6(3):115–20.
- [23] de Groot N, van der Does L, Yaksh A, Lanters E, Teuwen C, Knops P, et al. Direct proof of endo-epicardial asynchrony of the atrial wall during atrial fibrillation in humans. *Circ Arrhythm Electrophysiol* 2016;9(5).
- [24] de Groot NM, Houben RP, Smeets JL, Boersma E, Schotten U, Schalij MJ, et al. Electropathological substrate of longstanding persistent atrial fibrillation in patients with structural heart disease: epicardial breakthrough. *Circulation* 2010;122(17):1674–82.
- [25] Saraf K, Ariyaratnam J, Zaki A, Morris GM. Lateral epicardial breakthrough as a perpetuator of cavotricuspid isthmus conduction despite bidirectional mid-isthmus block: an important diagnostic role for high-density electro-anatomical mapping. *EP Europace* 2018;20(S1):i96.
- [26] Higuchi S, Shoda M, Iwanami Y, Yagishita D, Ejima K, Hagiwara N. Targeting an epicardial-endocardial breakthrough in a case with an intractable common atrial flutter using ultra-high-resolution three-dimensional mapping. *Pacing Clin Electrophysiol* 2018;41(9):1261–3.